Title
Comparison of methods for measuring longitudinal brain change in cognitive impairment and dementia

Journal
Neurobiology of Aging, 24(4)

ISSN
0197-4580

Authors
Cardenas, V A
Du, A T
Hardin, D
et al.

Publication Date
2003-07-01

Peer reviewed

ELSEVIER

Neurobiology of Aging 24 (2003) 537–544

NEUROBIOLOGY OF AGING

www.elsevier.com/locate/neuaging

Comparison of methods for measuring longitudinal brain change in cognitive impairment and dementia

V.A. Cardenas[a,b,*], A.T. Du[a,b], D. Hardin[a,b], F. Ezekiel[a,c], P. Weber[a,b], W.J. Jagust[f], H.C. Chui[g], N. Schuff[a,b], M.W. Weiner[a,b,c,d,e]

[a] *Department of Veterans Affairs Medical Center, Magnetic Resonance Unit, 4150 Clement Street (116R), San Francisco, CA 94121 USA*

[b] *Department of Radiology, University of California, San Francisco, CA, USA*

[c] *Department of Psychiatry, University of California, San Francisco, CA, USA*

[d] *Department of Neurology, University of California, San Francisco, CA,USA*

[e] *Department of Medicine, University of California, San Francisco, CA, USA*

[f] *Department of Neurology, University of California, Davis, CA, USA*

[g] *Department of Neurology, University of Southern California, Los Angeles, CA, USA*

Received 7 January 2002; received in revised form 18 June 2002; accepted 22 August 2002

Abstract

Purpose: The goal of this project was to compare MRI measures of hippocampal, entorhinal cortex (ERC), and whole brain longitudinal change in cognitively normal elderly controls (C), non-demented subjects with cognitive impairment (CI), and demented (D) subjects.

Methods: 16 C, 6 CI, and 7 D subjects of comparable age were studied with MRI twice, at least 1 year apart. Longitudinal change in total brain size was measured by several methods, including computerized segmentation, non-linear warping, and change in the fluid/tissue boundaries between cerebrospinal fluid (CSF) and brain. Change in hippocampal volume was measured by semi-automated methods, and ERC volumes were manually measured.

Results: The annual rate of atrophy was greater in D versus C and D versus CI for cortical gray matter (cGM) ($P = 0.009$ and 0.002), hippocampus ($P = 0.0001$ and 0.002), and for the change in the fluid/tissue boundary ($P = 0.03$ and 0.03). The annual rate of atrophy of ERC was greater in both CI and D versus C ($P = 0.01$ and 0.0002). No significant differences between groups were found using non-linear warping.

Conclusions: In CI, the greatest annual rates of atrophy were in ERC, while in D the greatest annual rates of atrophy were in hippocampus and cortex. Progressive ERC atrophy was observed with a greater degree of cognitive impairment, while hippocampal and cortical atrophy were only observed in demented subjects.

Keywords: Cognitive disorders/dementia; Neuroradiology; Image processing; Longitudinal

1. Introduction

Alzheimer's disease (AD) is associated with progressive neurofibrillary degeneration, beginning in the entorhinal cortex (ERC) [31] and hippocampus [38], and spreading to the neocortex [1]. Numerous investigators have observed atrophy of these regions among patients with clinically diagnosed AD, using a variety of structural neuroimaging studies [24,25,36,40,44]. Reduced hippocampal size is found among patients with mild cognitive impairment (who are at risk to convert to AD) [28], and non-demented subjects with a family history of AD or carrying at least one apolipoprotein epsilon 4 allele [41]. Baseline volumes of ERC, banks of the superior temporal sulcus, and anterior cingulate discriminate between those who do or do not subsequently develop cognitive decline [33], suggesting that the earliest and greatest changes occur in these regions.

Previous researchers [32,42–44] have used computerized segmentation methods in order to compare volumes of gray matter, white matter, and CSF between AD patients and controls. Reduced cortical gray matter (cGM) volumes and increased CSF volumes were associated with AD. AD

* Corresponding author. Tel.: +1-415-221-4810x4086, fax: +1-415-502-2110.
E-mail address: valerie@itsa.ucsf.edu (V.A. Cardenas).

0197-4580/02/$ – see front matter © 2002 Elsevier Science Inc. All rights reserved.
PII: S0197-4580(02)00130-6

patients also had greater volumes of abnormal white matter, which was associated with more severe dementia. Tissue segmentation, however, has not been used to measure progression of AD.

Longitudinal changes in brain structure have been measured using a variety of methods. Early CT studies showed progression of atrophy in AD [29,40]. Using manual tracing of serial MRI, Jack et al. found that annual volume loss of hippocampus and temporal horn was increased in AD compared to controls [27], and that rates of hippocampal volume loss decreased according to disease severity, i.e. AD > CI > controls [26]. However, manual hippocampal tracing is time-consuming and is potentially susceptible to operator bias.

The boundary shift integral (BSI) [18] is another measure of cerebral volume change that has been used to estimate longitudinal changes in dementia. BSI measures how the boundaries between solid brain tissue and cerebrospinal fluid (CSF) change between two scans. A major advantage of BSI over tracing methods is that no regions of interest need to be selected for measurements of longitudinal volume changes, thus providing an unbiased approach for identification of regions with progressive tissue loss. A series of studies [14–18] demonstrated that BSI detected substantially more tissue loss in AD patients than in cognitively normal elderly subjects, especially in regions of the temporal lobe, with no overlap between the two groups. However, fluid/tissue boundary shifts can be due to a variety of reasons, including tissue loss at the cortex and/or deep within the brain, or boundary deformations without tissue loss. In addition, BSI cannot localize the site of tissue atrophy.

Similar to BSI, non-linear warping methods [19,46] also provide measurements of regional tissue loss, without choosing regions of interest. Using non-linear warping, Freeborough and co-workers found greater atrophy in the temporal lobes of AD than controls, similar to results from BSI, while the cerebellum was relatively unchanged [7,19]. In contrast to BSI, however, some overlap between the groups remained. Toga et al. developed a tensor mapping technique to examine rates of atrophy in AD and controls and found faster rates of tissue loss in the left than in the right hippocampus [46]. Furthermore, rates of hippocampal atrophy correlated with cognitive decline.

Because previous longitudinal MRI studies applied different methods to different patient populations, it is difficult to compare the power of the different methods for differentiating groups with varying rates of cognitive decline. Furthermore, there are no MRI reports of longitudinal ERC change, although ERC is known to be involved early in the course of AD. Therefore, the goal of this project was to compare measures of ERC, hippocampal, and whole brain longitudinal change in cognitively normal elderly controls, nondemented subjects with cognitive impairment, and patients with AD.

2. Methods

2.1. Subjects

Subjects were recruited for a study that compared subjects with ischemic vascular dementia to cognitively normal subjects, cognitively impaired subjects, patients with AD, and patients with mixed vascular and Alzheimer's dementia. Subjects with multiple MRI scans separated by 1 or more years were included in this analysis. These 29 subjects were initially scanned between October 1994 and December 1997, and 1–4 years after their first scan. In addition to MRI, cognitive functions of the patients were generally tested within 3 months of the MRI scans (two patients tested within 6 months). Subjects were recruited through advertisement or referred by clinics in the San Francisco area, and were clinically evaluated at the Alzheimer's centers at the University of California, San Francisco and Davis. All subjects were evaluated at the Alzheimer's centers using a standard battery of neurological and neuropsychological tests as described previously [11]. Subjects were classified by a diagnostic team as cognitively normal (C) ($N = 16$, 6 women/10 men), cognitively impaired but not demented (CI) ($N = 6$, 0/6), or demented (D) ($N = 7$, 5 AD, 2 mixed AD and ischemic vascular dementia, 4/3), based on a comprehensive dementia evaluation that included history from the patients and a caregiver, neurological and mental status examinations of the patient, and neuropsychological testing. To be classified as CI, the neuropsychological testing determined that the patient's cognitive function was not normal, but that they did not meet DSM IV criteria for dementia. Examples of this situation would include a single, isolated cognitive deficit or a set of mild cognitive deficits insufficient to cause significant functional impairment. Neuropsychological testing was classified as normal or not according to the clinical judgment of neuropsychologists expert in the evaluation of dementia, and took into account all relevant factors including estimated premorbid functions. However, the final diagnosis was not solely based on the test interpretation. It was the consensus diagnosis of the clinicians based on all available evidence. Some CI patients did not meet the criteria for MCI published by Petersen et al. [35]. The subjects were of comparable age (mean ± standard deviation years): C (76 ± 5), CI (70 ± 9), and D (76 ± 8). The scan intervals (in years) between groups were also comparable: C (2.6 ± 1.0), CI (2.3 ± 0.8), and D (2.6 ± 1.0). None of the C or CI subjects converted to another group during the study period. Severity of cognitive impairment was assessed using the Folstein Mini-Mental State Exam (MMSE) [13]. Initial MMSE scores (maximum score: 30) for each group were: C (29.1 ± 1.0), CI (27.5 ± 2.4), and D (24.6 ± 2.6).

MRI data were acquired on a clinical 1.5 T MR scanner (Vision, Siemens Medical Systems, Iselin, NJ). The MRI protocol consisted of a double spin-echo (DSE) sequence, yielding proton density and T2 weighted MR images

and a Magnetization Prepared Rapid Acquisition Gradient Echo (MPRAGE) sequence, yielding T1-weighted MR images. Axially angulated DSE images (TR/TE1/TE2 = 2500/20/80 ms, 1.0 mm × 1.2 mm resolution, 3 mm slice thickness) were oriented along the optic nerve as seen in a sagittal scout image through the brain midsection, resulting in images approximately parallel to the long axis of the hippocampus. Coronal MPRAGE (TR/TI/TE = 9/300/4, 1 mm × 1 mm in-plane resolution, 1.5 mm slabs) were acquired orthogonal to DSE.

2.2. Tissue segmentation

Using tissue segmentation, we generated estimates of the annual rate of change for cGM, white matter, subcortical gray matter, sulcal CSF, ventricular CSF, and white matter signal hyperintensities (WMSH). Our tissue segmentation procedures are based on *k*-means cluster analysis of the PD, T2, and T1-weighted images, and have been described in detail elsewhere [2]. Using this segmentation method, test–retest reliabilities of tissue volume measurements as evaluated using an intraclass correlation coefficient (ICC, range 0–1.0 [12]) were greater than 0.95 for all tissue types except WMSH, where ICC was 0.80. Tissue segmentation was completed independently for the baseline and repeat scans for each subject, and angulation differences between scans were corrected to ensure that the change measures were computed for comparable regions. For each tissue type, the change measure was computed as

$$\frac{(\text{volume}_{\text{baseline}} - \text{volume}_{\text{repeat}})/\text{volume}_{\text{baseline}} \times 100\%}{\text{interscan interval in years}},$$

and reported as %atrophy per year.

2.3. Hippocampal voluming

We generated an estimate of the annual rate of hippocampal volume change from volume measurements of the left and right hippocampus, computed using a semi-automated method (Surgical Navigation Technologies (SNT), a Division of Medtronic, Boulder, CO). This method employs pattern matching techniques to map a hippocampal template from a normal elderly subject to each subject's hippocampus [4,9,21,22]. Using SNT, a subvolume of the T1-weighted scan (1.5 mm slices) containing the hippocampus is defined by using 22 landmarks that guide global matching of the hippocampus. Hippocampal volumes estimated using this method had high test–retest reliability; ICC = 0.98, 0.94, and 0.97 for left, right, and total hippocampus [23]. Each scan was independently marked by operators blinded to all clinical information and chronological scan order. A total hippocampal volume was obtained by summing the left and right volumes, and the annual rate was computed as described for the tissue segmentation, and reported as %atrophy per year.

2.4. Entorhinal cortex voluming

We generated an estimate of the annual rate of ERC volume change from volume measurements of the left and right entorhinal cortices, manually measured by drawing the boundary of the structures as seen in the coronal T1-weighted images according to the protocol developed by Insausti et al. [24]. An experienced radiologist (ATD), who was blinded to the diagnosis and all other clinical information, performed the volume measurements of ERC. Volumes of left and right side were combined for a total ERC volume measurement. Reliabilities of ERC volume measurements were ICC = 0.98, 0.97, and 0.99 for left, right, and total ERC, respectively.

2.5. Boundary shift integral

The BSI measures the total volume through which fluid/tissue boundaries of the brain have moved between longitudinal studies. In this paper, we divided the BSI volume change by the brain volume at the first scan to generate a measure of %atrophy per year of the total brain. BSI was accomplished by coregistering longitudinal scans using a rigid-body transformation, then generating a subtraction image. The subtraction image intensity is near zero in regions where the two scans are the same, with bright and dark pixels denoting areas where the fluid/tissue boundary has shifted between scans. These tissue gain and loss pixels in the subtraction image were integrated to generate an estimate of volume change. The BSI method was implemented on our T1-weighted images as described by Fox and co-workers [18], with two minor modifications. We did not calibrate our images for voxel size changes as described by Fox, because our magnet calibration records showed that our voxel size was very stable over time. Unlike Fox, we corrected images for intensity non-uniformity using an algorithm proposed by Sled et al. [39], because intensity variations induced by RF non-uniformity of the transmitter/receiver head coil may mimic boundary shifts in the subtraction images. Six subjects (2 C, 3 CI, and 1 D) had artifacts in the cortical region on the subtraction images, so we computed the BSI on the ventricular region only.

2.6. Warping

We generated an estimate of %atrophy per year of the whole brain by direct analysis of the non-linear transformation required to warp one image to match another voxel by voxel. In contrast to linear rigid-body transformations (such as those used in BSI) that account only for differences in position and rotation between images, non-linear transformations can allow brain regions to deform in order to match images. Many non-linear transformation techniques have been reported [3,5,6,20,45], and the Jacobian determinant of the transformation resulting from any of these methods then gives the percentage volume contraction or

expansion at each voxel as a result of the warping. In this paper, we explored the use of automated image registration (AIR 3.08) [47], a widely used image registration package, for non-linear registration. Using AIR 3.08, we warped the baseline T1-weighted images (1.5 mm slabs) to the repeat T1-weighted images, modeling the deformation field required to match the images as a fifth order polynomial. We computed the Jacobian of the transformation, then averaged (1.0-Jacobian) over all points in the brain divided by the interscan interval to compute a measure of %atrophy per year. When applied to the same test–retest set described above, an average 1.6% increase in total brain volume was estimated.

2.7. Statistics

The Wilcoxon Rank Sum test was used to evaluate rates of atrophy by group. Because we expected the magnitude of the rates of change to be ordered as D > CI > C, one-tailed tests were used. Because our samples were too small for more sophisticated statistical tests such as discriminant analysis, effect sizes [ES = |(mean 1 − mean 2)|/(0.5(SD 1 + SD 2))] for comparing pairwise combinations of groups were used in order to determine which methods best separated groups. We also used one-tailed *t*-tests to check whether our measures of longitudinal change were significantly different from zero.

3. Results

Table 1 shows the annual rates of change for each measure in C, CI, and D. Measures that were not significantly different between C and either CI or D are not displayed. Most measures of longitudinal change were significantly different from zero (i.e. atrophy or hypertrophy occurred over the scan interval). For C, there was no significant change as measured by total brain warping. For CI, there was no significant change as measured by warping, BSI, and segmentation of white matter, subcortical gray matter, and WMSH. For D, there was no significant change measured by warping or by segmentation of white matter and WMSH.

Fig. 1 illustrates the %atrophy per year for total hippocampus, gray matter, BSI at the ventricular fluid/tissue boundary, and total ERC as a function of group. This shows progressing rates of atrophy from controls to demented subjects for ERC voluming. Using hippocampal voluming, cGM segmentation, or BSI, controls and CI subjects had comparable rates of atrophy, and D subjects showed higher rates of atrophy.

There were no significant differences between groups when whole brain atrophy was measured via the non-linear warping methods (i.e. Jacobian of the AIR 3.08 polynomial transformation). There were also no significant differences for most of the segmentation tissue categories, other than cGM; white matter, subcortical gray matter, sulcal CSF, ventricular CSF, and WMSH were not significantly different between controls and CI or D.

3.1. Comparison of CI with C

The annual rate of total ERC atrophy was significantly greater in CI compared to controls (6.5% versus 2.6% atrophy per year, $P = 0.01$, ES = 1.12). In contrast to annual changes seen with MRI, changes of global cognitive functioning as assessed using MMSE scores over the interscan interval were not different between CI and C.

3.2. Comparison of D with C

D patients had significantly greater rates of atrophy than C for the measures shown in Table 1. There was a significantly greater rate of cGM atrophy in D compared to C as measured by segmentation (2.8% versus 0.9% atrophy per year, $P = 0.009$, ES = 1.19). There were also larger changes in the fluid/tissue boundary in D compared to C, as measured with BSI over the ventricular region (0.4% versus 0.2% atrophy per year, $P = 0.03$, ES = 1.00). The rate of total ERC atrophy (9.3 versus 2.6, $P = 0.0002$, ES = 2.03) was also much greater in D compared to C. The rate of total hippocampal

Table 1
Comparison of measures of longitudinal change

Measure	C ($N = 16$)	CI ($N = 6$)	D ($N = 7$)	ES: CI vs. C	ES: D vs. C	ES: D vs. CI
cGM	0.9 ± 1.4	0.6 ± 0.5	2.8 ± 1.8	0.22	1.19†	1.80†
Hippocampus	1.8 ± 0.8	1.9 ± 2.3	5.4 ± 2.8	0.06	1.96*	1.35‡
ERC	2.6 ± 2.2	6.5 ± 4.8	9.3 ± 4.4	1.12‡	2.03*	0.61
Brain: BSI[a]	0.2 ± 0.1	0.1 ± 0.2	0.4 ± 0.3	0.28	1.00‡	1.03‡
MMSE	−0.3 ± 1.6	2.4 ± 10.1	6.3 ± 5.9	0.45	1.74*	0.49

All measures reported as average %change per year ± standard deviation, where positive rate values represent decline. Statistical tests were one-sided Wilcoxon rank. C: control, CI: cognitively impaired, D: dementia, ES: effect size, ERC: entorhinal cortex, cGM: cortical gray matter.

[a] BSI computed from the shift at the ventricular boundary only.

* $P \leq 0.0008$.

† $P \leq 0.009$.

‡ $P \leq 0.03$.

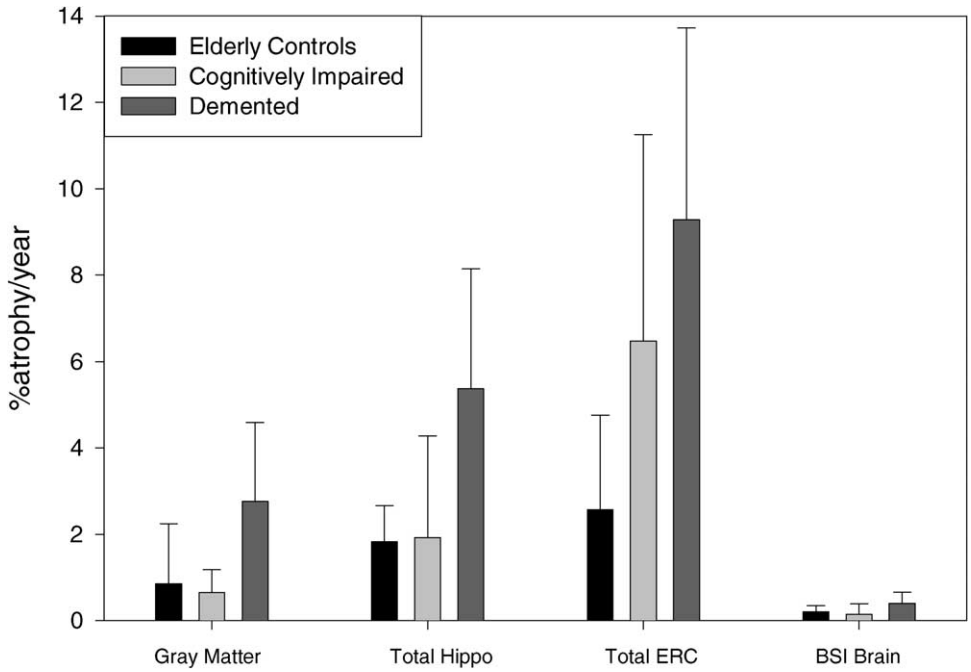

Fig. 1. Annual rate of atrophy (in percent) is shown for controls (C), subjects who are cognitively impaired but not demented (CI), and dementia subjects (D) for gray matter, total hippocampus (hippo), total entorhinal cortex (ERC), and brain as measured using the boundary shift integral (BSI) at the ventricular region.

(5.4 versus 1.8, $P = 0.0001$, ES $= 1.96$) atrophy was also much greater in D compared to C. The change in MMSE (expressed as %change per year) was also much larger in D compared to C (6.3% versus -0.3% change per year, $P = 0.0008$, ES $= 1.74$). Voluming of the hippocampus and ERC were the imaging measures that had the greatest ES.

3.3. Comparison of D with CI

The annual rate of total hippocampal atrophy was greater in D versus CI (5.4 versus 1.9, $P = 0.02$, ES $= 1.35$). There was a significantly greater rate of cGM atrophy in D compared to CI as measured by segmentation (2.8% versus 0.6% atrophy per year, $P = 0.002$, ES $= 1.80$). There were also larger changes in the fluid/tissue boundary in D compared to C, as measured with BSI over the ventricular region (0.4% versus 0.1% atrophy per year, $P = 0.03$, ES $= 1.03$). However, these results must be interpreted with caution, as we only had measurements on 7 D and 6 CI patients.

4. Discussion

The major findings of this study were that (1) annual rate of ERC atrophy was greater in CI than in C and (2) the annual rates of ERC, hippocampal, cortex (measured by cGM segmentation) or whole brain (measured by BSI) atrophy were greater in D than in C. Therefore, these results suggest that different spatial patterns of brain atrophy are associated with different severity of cognitive impairment. The finding in CI of greater annual rates of ERC atrophy than cGM loss is consistent with the generally accepted view that the ERC is an early site of impact by dementia, before pathology spreads to multi-modal association cortices in subsequent stages of the disease. However, the proportion of CI in this study that will ultimately develop AD and those with other forms of cognitive impairment, not associated with AD, is currently not clear. Therefore, these findings must be interpreted with care. Nevertheless, these results imply that when MRI is used as an outcome measure for experimental treatment trials of AD, the choice of regions of brain for study depends on the severity of cognitive impairment. Based on a comparison of ES, manual tracing of the ERC was the most sensitive measure for differentiating either D or CI from C. Another major finding of this study was that ERC and hippocampus were more sensitive measures of change than assessments of cognitive decline using MMSE.

Our main purpose in this paper was to use several methods to measure rates of atrophy on the same subjects, in order to determine the method most sensitive to group differences in longitudinal change. Based on our results, no single method is clearly superior. Instead, these results suggest that severity of cognitive impairment is associated with different patterns of longitudinal change. For example, CI subjects have a greater rate of ERC atrophy compared to controls, but are losing hippocampus and cortex at a similar rate to C subjects, while D subjects have greater rates of change everywhere we measured (cortex, hippocampus, ERC, and ventricles). Therefore, identifying patterns of

atrophy or determining relative rates of atrophy within a subject's brain may be more important diagnostically than a single measure of longitudinal change.

Previous work by Du et al. [10] showed that ERC volumes were reduced in CI and AD compared to normal controls (NC), such that ERC volume of AD < CI < NC. Although ERC volumes were not better discriminators of AD or CI from normal elderly controls than hippocampal volumes, consistent with findings from other MRI studies [28,30,34], they were better for differentiating CI versus AD. The present data show that the rate of ERC atrophy increases according to disease severity, i.e. C < CI < AD. Moreover, the largest magnitude in measurements of longitudinal change was ERC atrophy.

Although our BSI results detected differences between D and C, they were not as striking as those previously published. Previous work consistently reported rates of atrophy in controls of less than 0.5% per year and greater than 2% per year in AD patients [16,18], and also reported a correlation between BSI measures of atrophy and cognitive decline indexed by changing MMSE scores [17]. Our rates of atrophy in D were somewhat smaller, partly because we measured atrophy rate in the ventricular region only. We also suspect previous studies examined patients with more severe dementia than those reported here. In the previous work, MMSE scores of the AD group ranged from 8 to 28 with reported means of around 21. In our patients, the initial MMSE scores ranged from 20 to 27 and the mean was 24.6. It is possible that more severely demented patients have greater rates of atrophy as measured by BSI, which would help to explain these differences.

The failure of the warping method, AIR 3.08, to detect significant change may be due to limitations of this particular algorithm. This method estimated a 1.6% volume increase in our test-retest data where no volume change is expected, implying poor accuracy. The fifth order polynomial model of AIR 3.08 is very low dimensional, and is more appropriate for accounting for global differences in head size and shape across subjects than for estimating change within subjects. In order to detect longitudinal change in the same subjects, a higher dimensional warp is necessary so that small, localized areas of volume change can be modeled.

Although ERC and hippocampal atrophy were the most sensitive imaging measures of longitudinal change, measurements of both structures relied on manual methods that are subject to within and between rater errors. Future work will focus on methods to quantify regional longitudinal change using completely automated methods to eliminate rater involvement. Completely automated methods [8] to quantify longitudinal change should be very valuable for monitoring treatment effects in clinical trials, and possibly for improving the diagnosis of subjects in the early stages of AD.

There are several limitations to this study. A limitation of this study is that a very small sample of subjects was analyzed, increasing chances of making a Type II error when comparing rates of atrophy between groups of subjects. Chances of making a Type I error are also increased because group comparisons were repeated using different atrophy measurements. Therefore, any group differences in atrophy rates should be interpreted with caution, and we are currently gathering more longitudinal data so that we can verify our results on a larger sample. The major point of this paper is not so much to compare groups, which are admittedly small, but to compare different methods which measure rate of brain atrophy, between the same subjects. The statistical power of our results lies in the fact that one can directly compare measurements of hippocampus, ERC, gray matter, etc. in the same subjects, assuming that the most sensitive measurements of brain changes would be those that provide the largest separation between subjects.

Also, two of the D patients showed signs of ischemic subcortical strokes that are known to be associated with brain atrophy as well [11,37]. Therefore, our measurements of atrophy rate in D may be skewed to the extent that ischemic subcortical strokes contributed to volume losses. Another limitation is that segmentation was based on MRI data with a lower resolution than the other methods in this study, complicating the comparison with other methods. It is likely that the sensitivity of segmentation for measurement of atrophy rates improves at higher image resolution. Our segmentation algorithm also includes cerebellar gray matter in our cGM volumes. Since we do not expect significant longitudinal changes in cerebellar gray matter in dementia, its inclusion would most likely attenuate the cGM effect size between D and C.

In summary, this study showed that the greatest annual rates of atrophy in CI occurred in the ERC, and the greatest annual rates of cortical atrophy were in D patients, indicating regional variations in rate of brain atrophy for different stages of cognitive impairment. Thus, regional information is important when interpreting brain atrophy rates.

Acknowledgments

The authors wish to thank Diana Truran for overseeing segmentation of the images, Kevin Mark for assistance using SNT, Linda Rogers for statistical advice, and Nick Fox for helpful discussion concerning implementation of BSI. This work was supported by NIAAA P01AA11493 and NIA Grant AG12435.

References

[1] Braak H, Braak E. Staging of Alzheimer's disease-related neurofibrillary changes. Neurobiol Aging 1995;16(3):271–8.
[2] Cardenas VA, Ezekeil F, DiSclafani V, Gomberg B, Fein G. Reliability of tissue volumes and their spatial distribution for segmented magnetic resonance images. Psychiatr Res Neuroimaging 2001;106:193–205.

[3] Christensen GE. Consistent linear-elastic transformations for image matching. In: Proceedings of Information Processing in Medical Imaging; 1999, p. 224–37 [Ref. Type: Abstract].
[4] Christensen GE, Joshi SC, Miller MI. Volumetric transformation of brain anatomy. IEEE Trans Med Imaging 1997;16(6):864–77.
[5] Christensen GE, Rabbit RD, Miller MI. 3D brain mapping using a deformable neuroanatomy. Phys Med Biol 1994;39:609–18.
[6] Collins DL, Evans AC. Animal: validation and applications of non-linear registration-based segmentation. Int J Pattern Recog Artif Intell 1997;2(8):1271–94.
[7] Crum WR, Freeborough PA, Fox NC. The use of regional fast fluid registration of serial MRI to quantify local change in neurodegenerative disease. In: Proceedings of Medical Imaging Understanding and Analysis Conference; 1999.
[8] Crum W, Freeborough P, Fox N. The use of regional fast fluid registration of serial MRI to quantify local change in neurodegenerative disease. UK: Oxford; 1999.
[9] Csernansky JG, Joshi S, Wang L, Haller JW, Gado M, Miller JP, et al. Hippocampal morphometry in schizophrenia by high dimensional brain mapping. Proc Natl Acad Sci USA 1998;95(19): 11406–11.
[10] Du A, Schuff N, Amend D, Laakso MP, Hsu YY, Jagust WJ, et al. MRI of entorhinal cortex and hippocampus in mild cognitive impairment and Alzheimer's disease. J Neurol Neurosurg Psychiatr 2001;71:441–7.
[11] Fein G, Di SV, Tanabe J, Cardenas V, Weiner MW, Jagust WJ, et al. Hippocampal and cortical atrophy predict dementia in subcortical ischemic vascular disease. Neurology 2000;55(11):1626–35.
[12] Fleiss JL, Shrout PE. Approximate interval estimation for a certain intraclass correlation coefficient. Psychometrika 1978;43(2):259–62.
[13] Folstein MF, Folstein SE, McHugh PR. Mini-mental state. A practical method for grading the cognitive state of patients for the clinician. J Psychiatr Res 1975;12(3):189–98.
[14] Fox NC, Cousens S, Scahill R, Harvey RJ, Rossor MN. Using serial registered brain magnetic resonance imaging to measure disease progression in Alzheimer disease: power calculations and estimates of sample size to detect treatment effects [see comments]. Arch Neurol 2000;57(3):339–44.
[15] Fox NC, Freeborough PA. Brain atrophy progression measured from registered serial MRI: validation and application to Alzheimer's disease. J Mag Res Imaging 1997;7(6):1069–75.
[16] Fox NC, Freeborough PA, Rossor MN. Visualisation and quantification of rates of atrophy in Alzheimer's disease [see comments]. Lancet 1996;348(9020):94–7.
[17] Fox NC, Scahill RI, Crum WR, Rossor MN. Correlation between rates of brain atrophy and cognitive decline in AD [see comments]. Neurology 1999;52(8):1687–9.
[18] Freeborough PA, Fox NC. The boundary shift integral: an accurate and robust measure of cerebral volume changes from registered repeat MRI. IEEE Trans Med Imaging 1997;16(5):623–9.
[19] Freeborough PA, Fox NC. Modeling brain deformations in Alzheimer disease by fluid registration of serial 3D MR images. J Comput Assist Tomography 1998;22(5):838–43.
[20] Gee JC, Reivich M, Bajcsy R. Elastically deforming 3D atlas to match anatomical brain images. J Comput Assist Tomography 1993;17:225–36.
[21] Haller JW, Banerjee A, Christensen GE, Gado M, Joshi S, Miller MI, et al. Three-dimensional hippocampal MR morphometry with high-dimensional transformation of a neuroanatomic atlas. Radiology 1997;202(2):504–10.
[22] Haller JW, Christensen GE, Joshi SC, Newcomer JW, Miller MI, Csernansky JG, et al. Hippocampal MR imaging morphometry by means of general pattern matching. Radiology 1996;199(3):787–91.
[23] Hsu Y-Y, Schuff N, Du AT, Hardin D, Zhu X, Mark L, et al. Automated hippocampal MR volumetry in Alzheimer disease. J Mag Res Imaging 2002;16(3):305–10.
[24] Insausti R, Juottonen K, Soininen H, Insausti AM, Partanen K, Vainio P, et al. MR volumetric analysis of the human entorhinal, perirhinal, and temporopolar cortices. Am J Neuroradiol 1998;19(4): 659–71.
[25] Jack CRJ, Petersen RC, O'Brien PC, Tangalos EG. MR-based hippocampal volumetry in the diagnosis of Alzheimer's disease. Neurology 1992;42:183–8.
[26] Jack Jr CR, Petersen RC, Xu Y, O'Brien PC, Smith GE, Ivnik RJ, et al. Rates of hippocampal atrophy correlate with change in clinical status in aging and AD. Neurology 2000;55(4):484–9.
[27] Jack CR, Petersen RC, Xu Y, O'Brien PC, Smith GE, Ivnik RJ, et al. Rate of medial temporal lobe atrophy in typical aging and Alzheimer's disease. Neurology 1998;51(4):993–9 [Ref. Type: Magazine Article].
[28] Jack Jr CR, Petersen RC, Xu YC, O'Brien PC, Smith GE, Ivnik RJ, et al. Prediction of AD with MRI-based hippocampal volume in mild cognitive impairment. Neurology 1999;52(7):1397–403.
[29] Jobst KA, Smith AD, Szatmari M, Esiri MM, Jaskowski A, Hindley N, et al. Rapidly progressing atrophy of medial temporal lobe in Alzheimer's disease. Lancet 1994;343(8901):829–30.
[30] Juottonen K, Laakso MP, Partanen K, Soininen H. Comparative MR analysis of the entorhinal cortex and hippocampus in diagnosing Alzheimer disease. Ajnr Am J Neuroradiol 1999;20(1):139–44.
[31] Kesslak JP, Nalcioglu O, Cotman CW. Quantification of magnetic resonance scans for hippocampal and parahippocampal atrophy in Alzheimer's disease [see comments]. Neurology 1991;41:51–4.
[32] Kidron D, Black SE, Stanchev P, Buck B, Szalai JP, Parker J, et al. Quantitative MR volumetry in Alzheimer's disease. Topographic markers and the effects of sex and education. Neurology 1997;49(6):1504–12.
[33] Killiany RJ, Gomez-Isla T, Moss M, Kikinis R, Sandor T, Jolesz F, et al. Use of structural magnetic resonance imaging to predict who will get Alzheimer's disease. Ann Neurol 2000;47(4):430–9.
[34] Laakso MP, Frisoni GB, Kononen M, Mikkonen M, Beltramello A, Geroldi C, et al. Hippocampus and entorhinal cortex in frontotemporal dementia and Alzheimer's disease: a morphometric MRI study. Biol Psychiatr 2000;47(12):1056–63.
[35] Petersen RC, Stevens JC, Ganguli M, Tangalos EG, Cummings JL, DeKosky ST. Practice parameter: early detection of dementia: mild cognitive impairment (an evidence-based review). Neurology 2001;56:1133–42.
[36] Rombouts SA, Barkhof F, Witter MP, Scheltens P. Unbiased whole-brain analysis of gray matter loss in Alzheimer's disease. Neurosci Lett 2000;285(3):231–3.
[37] Schuff N, Du AT, Amend D, Jagust W, Yaffe K, Chui H, et al. MRI of entorhinal cortex and hippocampus in Alzheimer's disease, ischemic vascular dementia. In: Iqbal K, Sisodia SS, Winblad B, editors. Alzheimer's disease: advances in etiology, pathogenesis and therapeutics. New York: Wiley; 2001.
[38] Seab JP, Jagust WJ, Wong ST, Roos MS, Reed BR, Budinger TF. Quantitative NMR measurements of hippocampal atrophy in Alzheimer's disease. Mag Reson Med 1988;8:200–8.
[39] Sled JG, Zijdenbos AP, Evans AC. A non-parametric method for automatic correction of intensity non-uniformity in MRI data. IEEE Trans Med Imaging 1998;17(1):87–97.
[40] Smith AD, Jobst KA. Use of structural imaging to study the progression of Alzheimer's disease. Br Med Bull 1996;52(3):575–86.
[41] Soininen H, Partanen K, Pitkanen A, Hallikainen M, Hanninen T, Helisalmi S, et al. Decreased hippocampal volume asymmetry on MRIs in non-demented elderly subjects carrying the apolipoprotein E epsilon 4 allele. Neurology 1995;45:391–2.
[42] Stout JC, Bondi MW, Jernigan TL, Archibald SL, Delis DC, Salmon DP. Regional cerebral volume loss associated with verbal learning and memory in dementia of the Alzheimer type. Neuropsychology 1999;13(2):188–97.
[43] Stout JC, Jernigan TL, Archibald SL, Salmon DP. Association of dementia severity with cortical gray matter and abnormal white

matter volumes in dementia of the Alzheimer type. Arch Neurol 1996;53(8):742–9.
[44] Tanabe JL, Amend D, Schuff N, DiSclafani V, Ezekiel F, Norman D, et al. Tissue segmentation of the brain in Alzheimer disease. Ajnr Am J Neuroradiol 1997;18(1):115–23.
[45] Thompson P, Toga AW. A surface-based techniques for warping three-dimensional images of the brain. IEEE Trans Med Imaging 1996;15(4):402–17.
[46] Toga A, Thompson P, Mega M, Cummings J. Detecting dynamic (4D) profiles of degenerative rates in Alzheimer's disease patients, using tensor mapping and a population-based based atlas. New Orleans, LA; 2000.
[47] Woods RP, Grafton ST, Watson JD, Sicotte NL, Mazziotta JC. Automated image registration. II. Intersubject validation of linear and non-linear models. J Comput Assist Tomography 1998;22(1): 153–65.